*Water* **2015**, *7*, 3515-3530; doi:10.3390/w7073515

OPEN ACCESS

*water*

**ISSN 2073-4441**
www.mdpi.com/journal/water

*Article*

# Characterization of the Corrosive Action of Mineral Waters from Thermal Sources: A Case Study at Azores Archipelago, Portugal

**Helena Cristina Vasconcelos [1,2,*], Bibiana María Fernández-Pérez [3,†], Sergio González [3,†], Ricardo Manuel Souto [3,4,†] and Juan José Santana [5,†]**

1 Department of Technological Sciences and Development, University of the Azores, Ponta Delgada 9501-801, Portugal
2 Center of Research in Natural Resources (CIRN), University of the Azores, Ponta Delgada 9501-801, Portugal
3 Department of Chemistry, University of La Laguna, P.O. Box 456, La Laguna 38200, Tenerife, Spain; E-Mails: bibianamariafp@gmail.com (B.M.F.-P.); sjglez@ull.es (S.G.); rsouto@ull.es (R.M.S.)
4 Institute of Material Science and Nanotechnology, University of La Laguna, P.O. Box 456, La Laguna 38200, Tenerife, Canary Islands, Spain
5 Department of Process Engineering, University of Las Palmas de Gran Canaria, Las Palmas de Gran Canaria 35017, Gran Canaria, Spain; E-Mail: juan.santana@ulpgc.es

† These authors contributed equally to this work.

* Author to whom correspondence should be addressed; E-Mail: hcsv@uac.pt; Tel.: +351-296-650-172; Fax: +351-296-650-171.

Academic Editor: Maria Filomena Camões

*Received: 5 March 2015 / Accepted: 25 June 2015 / Published: 2 July 2015*

---

**Abstract:** Waters from natural sources of the São Miguel Island in the Azores archipelago have been investigated regarding their corrosive action on metallic materials. The corrosive and encrusting characteristics of the waters have been established in terms of relevant chemical parameters (namely pH, conductivity, total dissolved solids (TDS), and concentrations of bicarbonate, calcium, magnesium, chloride, and sulfate ions) and their temperature by using Langelier, Ryznar, Puckorius and Larson–Skold indexes. The validity of this methodology has been tested by measuring the corrosion rates of various metals exposed to various waters using electrochemical methods. The materials of industrial

interest under investigation were carbon and galvanized steel, zinc, 304 and 316L grade stainless steels, brass, and Cr–Ni alloys. The greater aggressiveness of these waters was found for the less noble materials, and they experienced high corrosion rates.

**Keywords:** mineral waters; thermal sources; corrosivity; encrusting power; analytical modelling; electrochemical testing

## 1. Introduction

The composition of the mineral waters from volcanic regions is influenced by the various geochemical processes involved in the eruptive processes that gave rise to the growth of the volcanic edifice. Thus, numerous hydrogeochemical studies of mineral waters in volcanic terrains can be found in the scientific literature, and they are generally focused either on the geochemical processes that explain the composition of the water with the volcano in dormant state, or the stress changes associated with episodes of eruption. Though examples of the application of hydrogeochemical studies of geothermal waters regarding the pollution of underground aquifers can be found in the scientific literature [1,2], studies concerning their effect on the performance of the structural materials employed in their extraction or exploitation, namely as for their corrosion action, are rather scarce.

In the Azores, a volcanic archipelago in the North Atlantic Ocean about 1500 km off the Portugal mainland, there are sources of mineral and thermal water in seven of the nine Islands (namely in São Miguel, Terceira, São Jorge, Pico, Faial, Graciosa, and Flores). The Azores stretch along 600 km in a NW–SE direction, between latitudes 36°55′43″ N and 39°43′23″ N and longitudes 24°46′15″ W and 31°16′24″ W, with a total surface area equivalent to 2333 km$^2$, and nearly a half million population. Due to the volcanic nature of the Azores, the geochemistry of ground water is affected by the dissolution of primary minerals from volcanic rocks. The release of the major ions depends on the saturation states of the primary minerals, the secondary minerals precipitation, the aqueous chemistry of each component that leads to the formation of both soluble and insoluble species, and the acid nature of the environment [3]. However, as in other areas, the chemical composition of groundwater also depends on other factors, such as chemical precipitation, climate, type of rock, the residence time of the water, the segmentation of rock, the temperature, and pressure [4]. Additional factors would encompass an anthropogenic input of variable magnitude, and in the case of islands or coastal regions, the interaction with seawater [5–7]. Furthermore, the contribution of the rocks to the composition of groundwater in the volcanic regions also depends enormously on the release of volatile compounds in depth [8,9]. In the Azores, numerous mineral and thermal waters show the influence of these various processes [10,11].

Though the high quality of the therapeutic properties of thermal waters of the Azores was first described in 1614, it has been in more recent times that several springs were developed as spas, improving the social and economic welfare of the area. As result of this interest, the chemical composition and the therapeutic uses of mineral waters, in particular those from the island of São Miguel, are currently investigated as evidenced by various publications in specialized journals over the last decade [12–16].

The existence of diverse quality water presents a problem when the goal is to design facilities for extraction or exploitation. Thus, given the great variability of the compositions of waters shown in the afore mentioned studies, there is the need for a broad characterization of their aggressiveness towards metals of wide use in facilities, as well as more noble alternatives that may be recommended in cases of very aggressive water, despite their higher cost. This work reports some preliminary studies on the characterization of the aggressiveness of various types of water springs, hot springs and drilled wells in the islands of São Miguel, Terceira, São Jorge, Faial, Pico, Graciosa and Flores in the archipelago of the Azores. Their aggressiveness was tested against various metallic materials, namely zinc, carbon steel, brass, stainless steels, and CrNi alloys using electrochemical methods. We have also explored the applicability of Langelier Saturation, Ryznar Stability, Puckorius Scaling, and Larson–Skold Indexes for the characterization of the corrosive characteristics of hot springs and boiling pools.

## 2. Experimental

The values of of Langelier, Ryznar, Puckorius and Larson–Skold indexes were determined for a total of 86 samples of hot spring waters (boiling pool (bp)), spring waters (spring (spr)), and water from drilled wells (dw) in the islands of São Miguel, Terceira, São Jorge, Faial, Pico, Graciosa and Flores (Azores archipelago). The geochemical data used in the calculations as well as the geographical distribution of the analyzed sources were taken from a previous work by Cruz *et al.* [16] originally conducted on 101 samples of water. Since the work contained a few incomplete analyses as well as data from smaller islands other than those covered in this work, the sample population was effectively reduced to 86 in this work.

### *2.1. Determination of the Langelier Saturation Index (LSI)*

The Langelier Saturation Index (LSI) was obtained from the following expression [17],

$$LSI = pH_A - pH_S \quad (1)$$

where $pH_A$ is the actual pH of the water, and $pH_S$ is the pH of saturation. Water at equilibrium neither dissolves, nor precipitates calcium carbonate, so it is then characterized by its saturation pH, called $pH_S$. This is determined using,

$$pH_S = (9.3 + A + B) - (C + D) \quad (2)$$

where A, B, C and D are coefficients that are estimated as follows:

$$A = (\log [TDS] - 1)/10 \quad (3)$$

$$B = -13.12 \times \log (°C + 273) + 34.55 \quad (4)$$

$$C = \log [Ca^{+2}] \quad (5)$$

$$D = \log [Alk] \quad (6)$$

In these equations, TDS is the total dissolved solids, expressed in $mg \cdot L^{-1}$; $Ca^{2+}$ is the concentration of Ca(II) ions expressed as $CaCO_3$, in $mg \cdot L^{-1}$; and Alk is the total alkalinity given in the equivalent $CaCO_3$, and expressed in $mg \cdot L^{-1}$.

If LSI = 0, the water is considered to be neutral or at chemical equilibrium. Otherwise, when LSI < 0, the water has the tendency to be corrosive, whereas for LSI > 0, the water is supersaturated with respect to calcium carbonate ($CaCO_3$) and scale forming may occur, presenting encrusting trend.

### *2.2. Determination of the Ryznar Stability Index (RSI)*

The Ryznar Stability Index (RSI) [18] is obtained from the following expression,

$$RSI = 2(pH_S) - pH_A \quad (7)$$

where $pH_S$ and $pH_A$ have the same meaning and are calculated in the same way as shown for the Langelier Saturation Index.

When RSI ranges between 4.0 and 5.0, the water is strongly encrusting; between 5.0 and 6.0, it is slightly encrusting; between 6.0 and 7.0, it is slightly encrusting or corrosive; between 7.0 and 7.5, it is significantly corrosive; between 7.5 and 9.0 is strongly corrosive; and, finally, if it has a value of 9.0 or higher, the water is unbearably corrosive.

### *2.3. Determination of the Puckorius Scaling Index (PSI)*

The Puckorius Scaling Index (PSI) [19,20] was determined from the following expression,

$$PSI = 2(pH_{EQ}) - pH_S \quad (8)$$

In this equation, $pH_S$ is estimated as indicated for the two previous cases, whereas:

$$pH_{EQ} = 1.465 \times \log [Alk] + 4.54 \quad (9)$$

If the *PSI* value is less than 4.5, the water has tendency to encrusting; for $4.5 \leq PSI \leq 6.5$, the water is located within an optimal range where no corrosion may occur; and if it has a value greater than 6.5, there is driving force to corrosion.

### *2.4. Determination of the Larson–Skold Index (LI)*

The Larson–Skold Index (LI) [21] is widely used to describe the corrosivity of water towards mild steel lines. It is obtained from the following expression,

$$LI = ([Cl^-] + [SO_4^{2-}])/([HCO_3^-] + [CO_3^{2-}]) \quad (10)$$

where the concentrations of each of the species involved in the formula should be expressed in milliequivalents per liter ($meq \cdot L^{-1}$).

If LI amounts less than 0.8, the water does not have corrosive character; if the index lies between $0.8 \leq LI \leq 1.2$, the water is corrosive, and when it is greater than 1.2, the water presents a high corrosive character.

### *2.5. Electrochemical Characterization*

In order to quantify the corrosive nature of the hot springs, electrochemical tests were performed on metallic samples of zinc, carbon steel, galvanized steel, stainless steel 304 and 316L, brass and Cr–Ni alloys. The experiments were performed while the metals were exposed to water samples from various

thermal springs in São Miguel Island. The measurements of the polarization resistance were performed using Tafel determination and cyclic voltammetry. To that end, the metallic plates were placed at the bottom of a flat electrochemical cell as depicted in Figure 1.

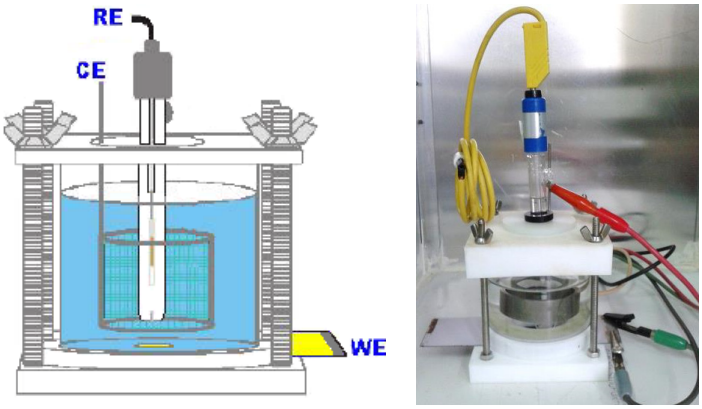


(**a**) (**b**)

**Figure 1.** Sketch (**a**) and photograph (**b**) of the electrochemical cell employed in this work.

Both the base and the lid were made from polyethylene, while the cylindrical side was from Pyrex glass. The base has a circular hole of about 6.5 $cm^2$ in area, allowing the direct exposure of the investigated metal to the water sample. Four screws on the sides and some o-rings allowed precise setting of the metal specimen without leakage. The electrochemical cell was operated in a configuration of three electrodes consisting of a working electrode (WE), which is the metal specimen under consideration, a saturated sodium chloride calomel electrode (SCE) operating as the reference electrode (RE, presenting a potential of +0.236 V with respect to the normal hydrogen electrode), and a counter electrode (CE) consisting of a stainless steel cylinder with a large surface area which is fixed to the top cover of the cell. The electrochemical cell and electrical connections were placed inside a grounded Faraday cage to isolate the system from external electromagnetic interferences. For the sake of comparison, all the measurements were performed in the naturally aerated waters and at ambient temperature (20 ± 1 °C).

Electrochemical measurements were performed using a potentiostat Model 2263 from Princeton Applied Research (AMETEK, Berwyn, PA, USA) under computer control. The tests were performed by shifting the potential ($E$) of the metal specimen from the open circuit potential ($E_{cor}$) developed by the material after 1 h immersion in the water sample, while recording the current density ($j$) flowing through the electrochemical cell. Polarization resistance measurements were conducted by sweeping the potential ±10 mV with respect to the $E_{cor}$ at a speed of 0.5 $mV \cdot s^{-1}$. Tafel plots were recorded by applying a potential sweep of ±200 mV *vs.* $E_{cor}$ at a speed of 2 $mV \cdot s^{-1}$. Finally, cyclic polarization curves were recorded in the potential $-0.1 \leq E \leq +0.8$ V *vs.* SCE, at a speed of 5 $mV \cdot s^{-1}$.

## 3. Results and Discussion

### *3.1. Estimation of the Corrosive Action of the Natural Waters Using Stability and Scaling Indexes*

Stability and scaling indexes were determined for natural waters from 86 locations across the Azores Islands by using their geochemical characteristics recorded by Cruz *et al.* [16]. They are

expressed in terms of the Langelier Saturation Index (LSI), Ryznar Stability Index (RSI), Puckorius Scaling Index (PSI), and the Larson–Skold Index (LI). The water sources were grouped according to their type as boiling pools (bp), spring (spr) and drilled well (dw). The physicochemical characteristics of the waters and their corresponding index values are listed in Tables 1–3. The water sources have been organized according to their type in the following categories: boiling pools (bp), springs (spr), and drilled wells (dw).

**Table 1.** Temperature, pH, conductivity (κ), total dissolved solids (TDS) and major element composition of mineral water from boiling pool (bp) discharges in the Azores archipelago according to Cruz *et al.* [16]. Calculation of the corresponding stability and scaling indexes, namely the Langelier Saturation Index (LSI), Ryznar Stability Index (RSI), Puckorius Scaling Index (PSI) and the Larson–Skold Index (LI).

| Water Source | *T*/°C | pH | κ/ $\mu S \cdot cm^{-1}$ | TDS/ $mg \cdot L^{-1}$ | $[Ca^{2+}]$/ $mg \cdot L^{-1}$ | $[SO_4^{2-}]$/ $mg \cdot L^{-1}$ | $[Cl^-]$/ $mg \cdot L^{-1}$ | $[HCO_3^-]$/ $mg \cdot L^{-1}$ | LSI | RSI | PSI | LI |
|---|---|---|---|---|---|---|---|---|---|---|---|---|
| **AM9** | 99.5 | 7.71 | 2010 | 1274 | 1.4 | 63 | 297.1 | 771 | 0.50 | 6.60 | 5.60 | 0.80 |
| **AM10** | 98.8 | 7.06 | 2350 | 1655 | 1.2 | 297 | 303.9 | 679.5 | −0.30 | 7.60 | 6.00 | 1.30 |
| **AM13** | 98.5 | 5.76 | 715 | 709 | 10 | 223 | 23.8 | 12.8 | −2.30 | 10.40 | 10.00 | 25.30 |
| **AM35** | 98 | 7.29 | 1785 | 1146 | 2.2 | 64 | 219 | 706.4 | 0.30 | 6.80 | 5.40 | 0.60 |
| **AM39** | 70 | 5.37 | 301 | 539 | 6.6 | 31 | 22.7 | 89.1 | −2.50 | 10.40 | 8.40 | 0.90 |

**Table 2.** Temperature, pH, conductivity (κ), total dissolved solids (TDS) and major element composition of mineral water from spring (spr) discharges in the Azores archipelago according to Cruz *et al.* [16]. Calculation of the corresponding stability and scaling indexes, namely the Langelier Saturation Index (LSI), Ryznar Stability Index (RSI), Puckorius Scaling Index (PSI), and the Larson–Skold Index (LI).

| Water Source | *T*/°C | pH | κ/ $\mu S \cdot cm^{-1}$ | TDS/ $mg \cdot L^{-1}$ | $[Ca^{2+}]$/ $mg \cdot L^{-1}$ | $[SO_4^{2-}]$/ $mg \cdot L^{-1}$ | $[Cl^-]$/ $mg \cdot L^{-1}$ | $[HCO_3^-]$/ $mg \cdot L^{-1}$ | LSI | RSI | PSI | LI |
|---|---|---|---|---|---|---|---|---|---|---|---|---|
| **AM1** | 21.1 | 5.27 | 410 | 814 | 9.6 | 46 | 22.7 | 120.8 | −3.20 | 11.70 | 9.40 | 0.60 |
| **AM2** | 34.4 | 5.33 | 365 | 619 | 11 | 41 | 19.9 | 159.2 | −2.70 | 10.70 | 8.30 | 0.50 |
| **AM3** | 75.1 | 6.16 | 515 | 416 | 8.9 | 7.5 | 36.9 | 256.8 | −1.00 | 8.20 | 6.30 | 0.30 |
| **AM4** | 15.9 | 5.09 | 301 | 840.1 | 8.2 | 18 | 20.9 | 92.1 | −3.70 | 12.50 | 10.10 | 0.60 |
| **AM5** | 15.6 | 4.95 | 306 | 697.3 | 11 | 33 | 19.5 | 74.4 | −3.80 | 12.50 | 10.20 | 1.00 |
| **AM6** | 16.2 | 4.99 | 210 | 767.9 | 11 | 32 | 24.5 | 72 | −3.80 | 12.50 | 10.20 | 1.10 |
| **AM7** | 41.3 | 5.57 | 522 | 738.7 | 11 | 13 | 59.3 | 226.9 | −2.20 | 10.00 | 7.50 | 0.50 |
| **AM8** | 40.4 | 5.58 | 519 | 728.5 | 9.5 | 11 | 65.3 | 228.1 | −2.30 | 10.10 | 7.70 | 0.60 |
| **AM11** | 59.5 | 6.21 | 1356 | 953 | 28 | 16 | 76.3 | 779.6 | −0.30 | 6.80 | 4.20 | 0.20 |
| **AM12** | 59.3 | 6.24 | 1271 | 939.8 | 30 | 18 | 76.3 | 767.4 | −0.30 | 6.70 | 4.20 | 0.20 |
| **AM14** | 17.5 | 6.77 | 190 | 159.1 | 4.5 | 6.2 | 18.5 | 80.5 | −2.20 | 11.20 | 10.60 | 0.50 |
| **AM15** | 41.3 | 6.02 | 1459 | 1117 | 28 | 14 | 91.9 | 786.9 | −0.80 | 7.70 | 4.90 | 0.20 |
| **AM16** | 42.7 | 6 | 1490 | 1250 | 30 | 19 | 88.8 | 889.4 | −0.70 | 7.50 | 4.60 | 0.20 |
| **AM17** | 42.5 | 6 | 1552 | 1305 | 34 | 16 | 90.1 | 865 | −0.70 | 7.40 | 4.50 | 0.20 |
| **AM18** | 47 | 6.14 | 1528 | 1250 | 40 | 9.7 | 96.6 | 932.1 | −0.40 | 6.90 | 4.10 | 0.20 |
| **AM19** | 41.2 | 6.25 | 1680 | 1259 | 43 | 12 | 100.8 | 1,091 | −0.30 | 6.80 | 4.00 | 0.20 |
| **AM20** | 39 | 5.85 | 587 | 414 | 20.3 | 10.5 | 57.2 | 247.7 | −1.60 | 9.10 | 6.90 | 0.50 |

**Table 2.** *Cont.*

| Water Source | *T*/°C | pH | κ/ μS·cm$^{-1}$ | TDS/ mg·L$^{-1}$ | [$Ca^{2+}$]/ mg·L$^{-1}$ | [$SO_4^{2-}$]/ mg·L$^{-1}$ | [$Cl^-$]/ mg·L$^{-1}$ | [$HCO_3^-$]/ mg·L$^{-1}$ | LSI | RSI | PSI | LI |
|---|---|---|---|---|---|---|---|---|---|---|---|---|
| **AM21** | 34.9 | 6.14 | 1759 | 1551 | 57 | 7 | 66.74 | 1161 | −0.40 | 6.80 | 4.00 | 0.10 |
| **AM21** | 34.9 | 6.14 | 1759 | 1551 | 57 | 7 | 66.74 | 1161 | −0.40 | 6.80 | 4.00 | 0.10 |
| **AM22** | 39 | 6 | 1,530 | 826.2 | 54 | 8.8 | 62 | 1080 | −0.40 | 6.90 | 3.90 | 0.10 |
| **AM23** | 32.9 | 6.02 | 1525 | 1388 | 58 | 14 | 67.1 | 1078 | −0.50 | 7.10 | 4.10 | 0.10 |
| **AM25** | 52.3 | 6.06 | 1441 | 1177 | 33 | 9.9 | 73.84 | 780.8 | −0.50 | 7.10 | 4.40 | 0.20 |
| **AM26** | 95.8 | 6.88 | 846 | 641.2 | 12.8 | 56 | 26.98 | 485.6 | 0.40 | 6.00 | 4.40 | 2.00 |
| **AM27** | 15.4 | 4.69 | 192 | 981 | 5.5 | 2.3 | 16.33 | 29.89 | −4.80 | 14.20 | 12.20 | 1.00 |
| **AM28** | 26.5 | 5.85 | 538 | 410.5 | 14.1 | 10 | 38.34 | 247.7 | −2.00 | 9.90 | 7.70 | 0.30 |
| **AM29** | 25.9 | 5.8 | 716 | 621.4 | 20 | 9.1 | 40.83 | 378.2 | −1.80 | 9.30 | 6.80 | 0.20 |
| **AM31** | 20.4 | 5.78 | 520 | 669.2 | 22 | 8.9 | 31.2 | 253.8 | −2.00 | 9.80 | 7.50 | 0.30 |
| **AM32** | 37.5 | 5.61 | 572 | 842 | 8.5 | 7.1 | 33.4 | 294 | −2.20 | 10.10 | 7.50 | 0.20 |
| **AM33** | 17.5 | 4.9 | 187 | 681.6 | 11 | 2.4 | 23.1 | 79.3 | −3.80 | 12.40 | 10.00 | 0.50 |
| **AM34** | 55.4 | 5.91 | 789 | 747 | 15 | 63 | 35.5 | 377 | −1.20 | 8.40 | 6.00 | 0.40 |
| **AM36** | 95.5 | 7.44 | 994 | 733 | 6.1 | 21 | 96.6 | 416 | 0.60 | 6.20 | 5.30 | 0.50 |
| **AM37** | 16.1 | 5.28 | 308 | 1353 | 7.8 | 27 | 19.9 | 78.1 | −3.60 | 12.50 | 10.50 | 0.90 |
| **AM38** | 16 | 4.89 | 356 | 1196 | 6.3 | 33 | 23.4 | 72 | −4.10 | 13.10 | 10.80 | 1.10 |
| **AM41** | 23.4 | 5.48 | 906 | 1524 | 77 | 92 | 80.94 | 336.7 | −1.60 | 8.80 | 6.00 | 0.80 |
| **AM42** | 32.8 | 7.58 | 1339 | 801 | 55 | 71 | 177.2 | 483.1 | 0.70 | 6.20 | 5.30 | 0.80 |
| **AM43** | 45.9 | 6.46 | 1239 | 895 | 57 | 63 | 133.8 | 599.0 | −0.10 | 6.60 | 4.50 | 0.50 |
| **AM44** | 18.6 | 5.71 | 1167 | 1456 | 35 | 15 | 70.65 | 684.4 | −1.40 | 8.60 | 5.60 | 0.20 |
| **AM45** | 17.9 | 5.3 | 377 | 979.3 | 16.7 | 2.1 | 26.63 | 170.2 | −2.90 | 11.00 | 8.50 | 0.30 |
| **AM46** | 15 | 4.87 | 139 | 949.9 | 8.8 | 6.2 | 16.68 | 67.1 | −4.00 | 12.90 | 10.60 | 0.50 |
| **AM47** | 17.4 | 5.2 | 326 | 747.2 | 5.6 | 13 | 47.2 | 65.9 | −3.80 | 12.90 | 10.90 | 1.50 |
| **AM48** | 18.1 | 4.66 | 184 | 1010 | 4.1 | 6 | 30.18 | 23.18 | −5.00 | 14.60 | 12.70 | 2.60 |
| **AM49** | 15.2 | 4.99 | 158 | 519.8 | 4 | 5.7 | 25.92 | 27.45 | −4.60 | 14.20 | 12.60 | 1.90 |
| **AM50** | 18.6 | 4.61 | 179 | 831.3 | 3.6 | 5.6 | 25.2 | 21.96 | −5.10 | 14.80 | 12.90 | 2.30 |
| **AM51** | 30 | 5.03 | 295 | 473.2 | 9.5 | 5.6 | 32 | 111 | −3.30 | 11.60 | 9.10 | 0.60 |
| **AM52** | 34.7 | 5.12 | 459 | 1077 | 11.1 | 6 | 53.3 | 176.9 | −2.90 | 10.90 | 8.20 | 0.60 |
| **AM53** | 19.4 | 4.8 | 194 | 1,070 | 3.7 | 4.6 | 33.02 | 23.18 | −4.90 | 14.50 | 12.80 | 2.70 |
| **AM54** | 70.3 | 5.98 | 360 | 386 | 8.9 | 19.5 | 35.14 | 88.45 | −1.80 | 9.50 | 8.10 | 1.00 |
| **AM55** | 16.5 | 5.09 | 330 | 1367 | 5.9 | 24 | 18.5 | 275.7 | −3.40 | 11.80 | 8.80 | 0.20 |
| **AM61** | 28.8 | 4.66 | 264 | 1041 | 4.6 | 56 | 23.8 | 29.3 | −4.60 | 13.90 | 11.90 | 3.80 |
| **AM62** | 36.2 | 4.28 | 182 | 544 | 3.9 | 31 | 20.9 | 28.1 | −4.90 | 14.10 | 11.70 | 2.70 |
| **AM69** | 18.5 | 4.65 | 326 | 1061 | 6.5 | 6.7 | 60.4 | 18.3 | −4.90 | 14.40 | 12.70 | 6.10 |
| **AM71** | 67.7 | 5.97 | 4,220 | 85,440 | 500 | 1,814 | 4,009 | 553.9 | 0.50 | 5.90 | 2.40 | 16.60 |
| **AM75** | 43 | 5.78 | 20,200 | 14,076 | 240 | 797 | 7455 | 596.6 | −0.30 | 6.40 | 3.60 | 23.20 |
| **AM76** | 32.8 | 6.36 | 20,140 | 7,953 | 140 | 352 | 4012 | 608.8 | −0.10 | 6.60 | 4.40 | 12.10 |
| **AM78** | 16 | 6.86 | 3980 | 2,523 | 44.5 | 184.5 | 1317 | 84.8 | −1.30 | 9.40 | 8.90 | 29.50 |
| **AM82** | 39.7 | 6.85 | 10,140 | 6778 | 174 | 228 | 3128 | 963.8 | 0.80 | 5.30 | 3.20 | 5.90 |
| **AM83** | 53.2 | 6.37 | 43,100 | 20,932 | 683 | 1,460 | 8821 | 712.5 | 1.00 | 4.40 | 2.10 | 23.90 |
| **AM84** | 38.6 | 6.75 | 13,100 | 6754 | 83 | 460 | 3,419 | 754 | 0.20 | 6.30 | 4.30 | 8.60 |
| **AM86** | 24.1 | 6.74 | 1234 | 826.7 | 67 | 6.5 | 47.6 | 707.6 | −0.10 | 6.90 | 4.90 | 0.10 |

**Table 2.** *Cont.*

| Water Source | *T*/°C | pH | κ/ μS·cm$^{-1}$ | TDS/ mg·L$^{-1}$ | [$Ca^{2+}$]/ mg·L$^{-1}$ | [$SO_4^{2-}$]/ mg·L$^{-1}$ | [$Cl^-$]/ mg·L$^{-1}$ | [$HCO_3^-$]/ mg·L$^{-1}$ | LSI | RSI | PSI | LI |
|---|---|---|---|---|---|---|---|---|---|---|---|---|
| **AM87** | 46.5 | 6.68 | 1244 | 745.9 | 47 | 50 | 95.8 | 577.1 | 0.00 | 6.60 | 4.70 | 0.40 |
| **AM89** | 20.5 | 5.69 | 10,210 | 5,761 | 91 | 435 | 3,220 | 658.8 | −1.20 | 8.00 | 5.10 | 9.20 |
| **AM90** | 20.9 | 5.79 | 1334 | 1118 | 16 | 49 | 300.3 | 154.9 | −2.40 | 10.50 | 8.60 | 3.70 |
| **AM94** | 15.5 | 5.76 | 203 | 220.9 | 9 | 3.5 | 23.1 | 72.4 | −3.00 | 11.80 | 10.30 | 0.60 |
| **AM95** | 15 | 5.35 | 192 | 322.3 | 9.2 | 4 | 21.6 | 61 | −3.50 | 12.40 | 10.6 | 0.70 |
| **AM99** | 35.1 | 6.09 | 6570 | 4310 | 111 | 194 | 2,016 | 426.4 | −0.60 | 7.30 | 5.00 | 8.70 |
| **AM100** | 18 | 6.05 | 9440 | 6,316 | 195 | 95.94 | 3,337 | 405.0 | −0.70 | 7.50 | 5.20 | 14.50 |

**Table 3.** Temperature, pH, conductivity (κ), total dissolved solids (TDS) and major element composition of mineral water from drilled well (dw) discharges in the Azores archipelago according to Cruz *et al.* [16]. Calculation of the corresponding stability and scaling indexes, namely the Langelier Saturation Index (LSI), Ryznar Stability Index (RSI), Puckorius Scaling Index (PSI), and the Larson–Skold Index (LI).

| Water Source | *T*/°C | pH | κ/ μS·cm$^{-1}$ | TDS/ mg·L$^{-1}$ | [$Ca^{2+}$]/ mg·L$^{-1}$ | [$SO_4^{2-}$]/ mg·L$^{-1}$ | [$Cl^-$]/ mg·L$^{-1}$ | [$HCO_3^-$]/ mg·L$^{-1}$ | LSI | RSI | PSI | LI |
|---|---|---|---|---|---|---|---|---|---|---|---|---|
| **AM56** | 22.5 | 5.27 | 537 | 1292 | 10.8 | 5 | 18.8 | 279.4 | −2.80 | 10.80 | 8.00 | 0.10 |
| **AM57** | 20.3 | 5.48 | 575 | 795.9 | 12.3 | 3.4 | 17.8 | 347.7 | −2.40 | 10.40 | 7.60 | 0.10 |
| **AM64** | 31.1 | 6.36 | 2090 | 1395 | 20 | 71 | 446.9 | 361.1 | −1.20 | 8.70 | 6.80 | 2.40 |
| **AM66** | 17 | 6.15 | 403 | 400.2 | 8.2 | 9.8 | 32.31 | 87.84 | −2.60 | 11.30 | 10.10 | 0.80 |
| **AM67** | 27.5 | 5.6 | 590 | 728.8 | 20 | 5.7 | 55.38 | 229.4 | −2.20 | 9.90 | 7.50 | 0.40 |
| **AM68** | 26 | 5.27 | 394 | 949.1 | 12.2 | 13.3 | 51.5 | 117.7 | −3.00 | 11.30 | 9.00 | 0.90 |
| **AM73** | 58 | 6.1 | 27,000 | 19,299 | 310 | 1120 | 10.50 | 608 | 0.40 | 5.40 | 2.80 | 32.10 |
| **AM74** | 57 | 6.2 | 28,000 | 19,672 | 317 | 1118 | 10.63 | 617 | 0.20 | 5.80 | 3.80 | 62.20 |
| **AM80** | 27.5 | 7.82 | 1153 | 564.3 | 25 | 29 | 277.2 | 81.7 | −0.30 | 8.40 | 8.90 | 6.30 |
| **AM81** | 36.3 | 6.4 | 42,000 | 29,127 | 630 | 1450 | 16,200 | 1226 | 0.90 | 4.70 | 2.00 | 24.20 |
| **AM101** | 39 | 6.04 | 7440 | 5102 | 183 | 226.6 | 2336 | 402.6 | −0.40 | 6.80 | 4.50 | 10.70 |

The analysis of the Langelier Saturation Index values for the five bp-type sources allow calculating the difference between the pH and the pH of saturation at which calco-carbonic equilibrium is achieved. It is observed that AM9 and AM35 sources present encrusting trend, while the other three sources have a corrosive trend, which corresponds to 60% of bp waters analyzed. While it is true that this index denotes a trend and not a speed, is evident the corrosive nature of these waters. The corrosive or encrusting character can be affected by the high temperatures occurring in these water sources. Though the temperature of the water is taken into account for the calculation of both the Langelier Saturation Index and the Ryznar Stability Index, as it reaches values close to the boiling point in some cases, the corrosive or encrusting process can be altered considerably. In some cases, a fixed temperature limit of 80 °C was taken for the estimation of the rates.

From the values obtained for the Ryznar Stability Index, it can be concluded that all the analyzed waters from boiling pools have corrosive character, (*i.e.*, RSI > 6), where two of them are unbearably corrosive (AM13 and AM39), while the Puckorius Scaling Index only attributes corrosive character to AM13 and AM19 sources. In the determination of these indexes, it has been estimated that the

concentration of carbonate in the samples was negligible due to their pH values. From an equilibrium graph of $CO_2$–$HCO_3^-$–$CO_3^{2-}$ as a function of pH [22], the concentration of ion $CO_3^{2-}$ should be less than $10^{-5}$ mol·L$^{-1}$ for the entire pH range covered in this work, where the highest value is 7.82 at AM80.

The risk of corrosive attack from pitting in carbon steel can be predicted using the Larson–Skold Index, where the chloride and sulfate ions are regarded to be the species responsible for the aggressive characteristics of the waters. According to this index, four of the boiling pool waters would promote corrosion, two of them presenting very high driving forces towards corrosion.

Analogously, the analysis of waters type spr according to the Langelier Saturation Index gives that more than 87.7% of the analyzed waters are prone to corrosion, 10.8% have tendency to encrustation, and only one of the waters presents chemical equilibrium (AM87). According to the Ryznar Stability Index, the corrosive ratio rises to more than 95.4% of the analyzed waters, from which 23.1% present light corrosive character, 6.2% a significant corrosive character, 12.3% a strong corrosive character, and 53.8% intolerable corrosive character.

The estimation of corrosivity using the Larson–Skold index, exclusively in terms of chloride and sulfate contents in the waters, led to the estimation that 35.3% of the water sources present corrosive characteristics, and 19.6% of them present a highly corrosive character. Thirdly, for the waters obtained from drained wells (dw), 72.7% are prone to corrosion according to both the Langelier Saturation Index and the Ryznar Stability Index. According to the latter, more than 63% of the waters present a strongly corrosive character, with 45% of them showing unbearably high corrosive character.

For the sake of comparison, Figures 2 to 5 illustrate the distribution of the water sources under consideration against the various stability and scaling indexes used in this work. The high aggressiveness of the waters present in these geothermal water sources is readily observable from the inspection of these graphs.

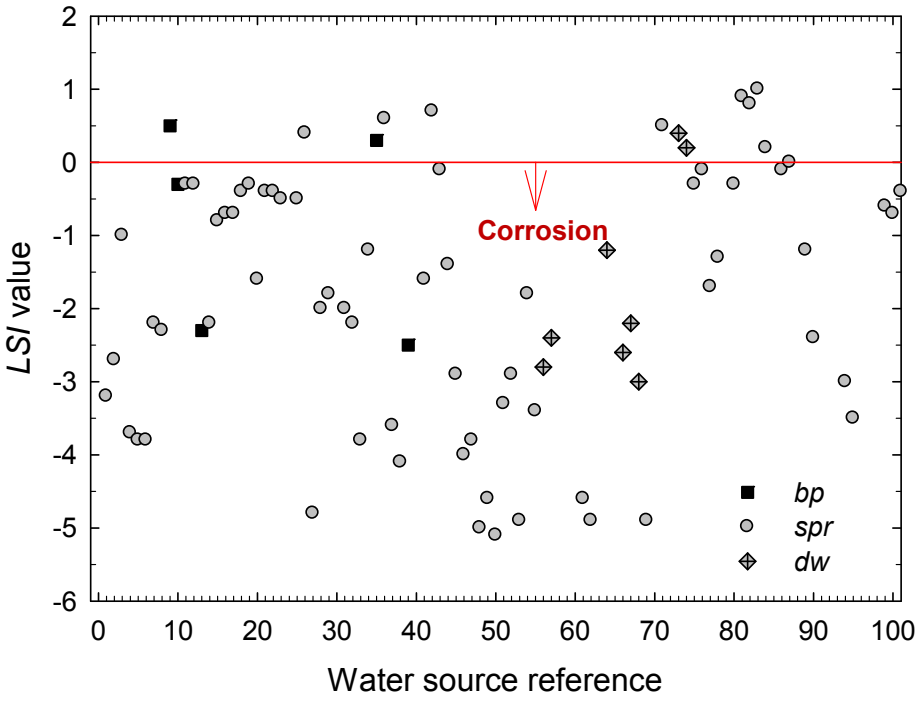


**Figure 2.** Distribution of the water sources in the Azores archipelago according to their Langelier Saturation Index (LSI).

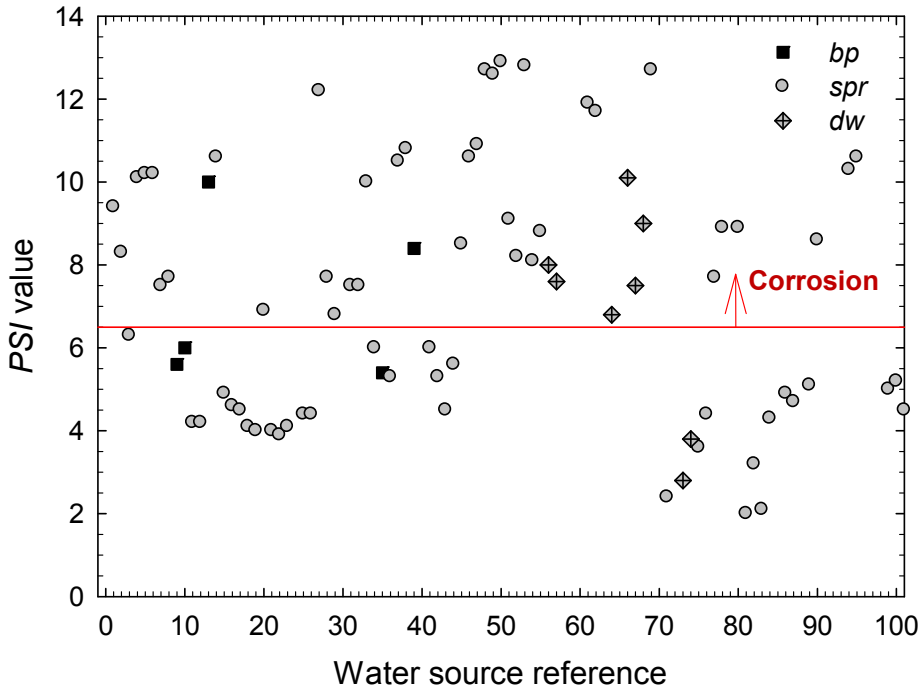


**Figure 3.** Distribution of the water sources in the Azores archipelago according to their Puckorius Scaling Index (PSI).

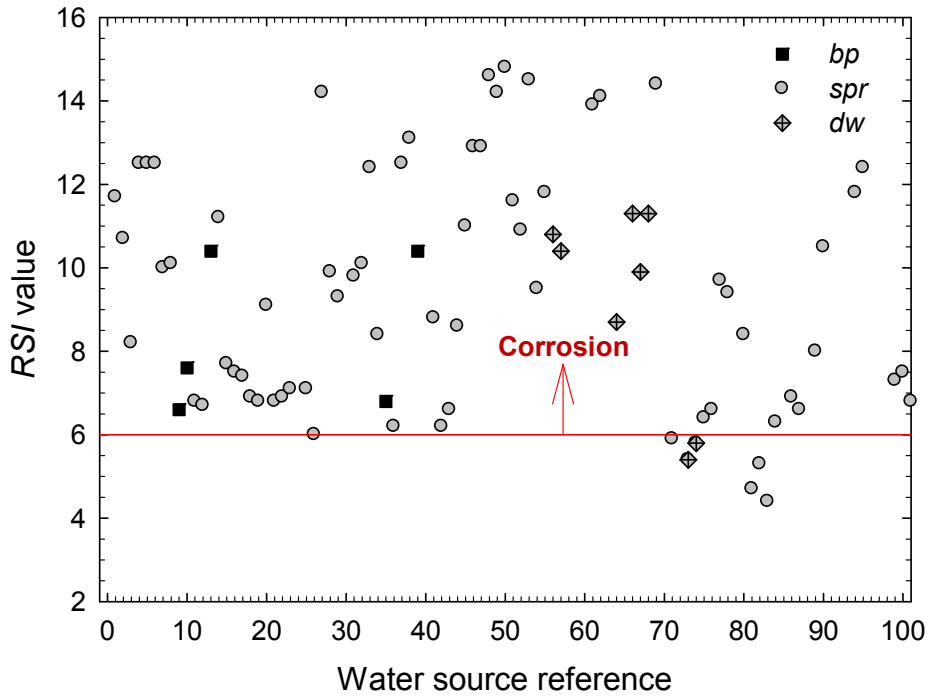


**Figure 4.** Distribution of the water sources in the Azores archipelago according to their Ryznar Stability Index (RSI).

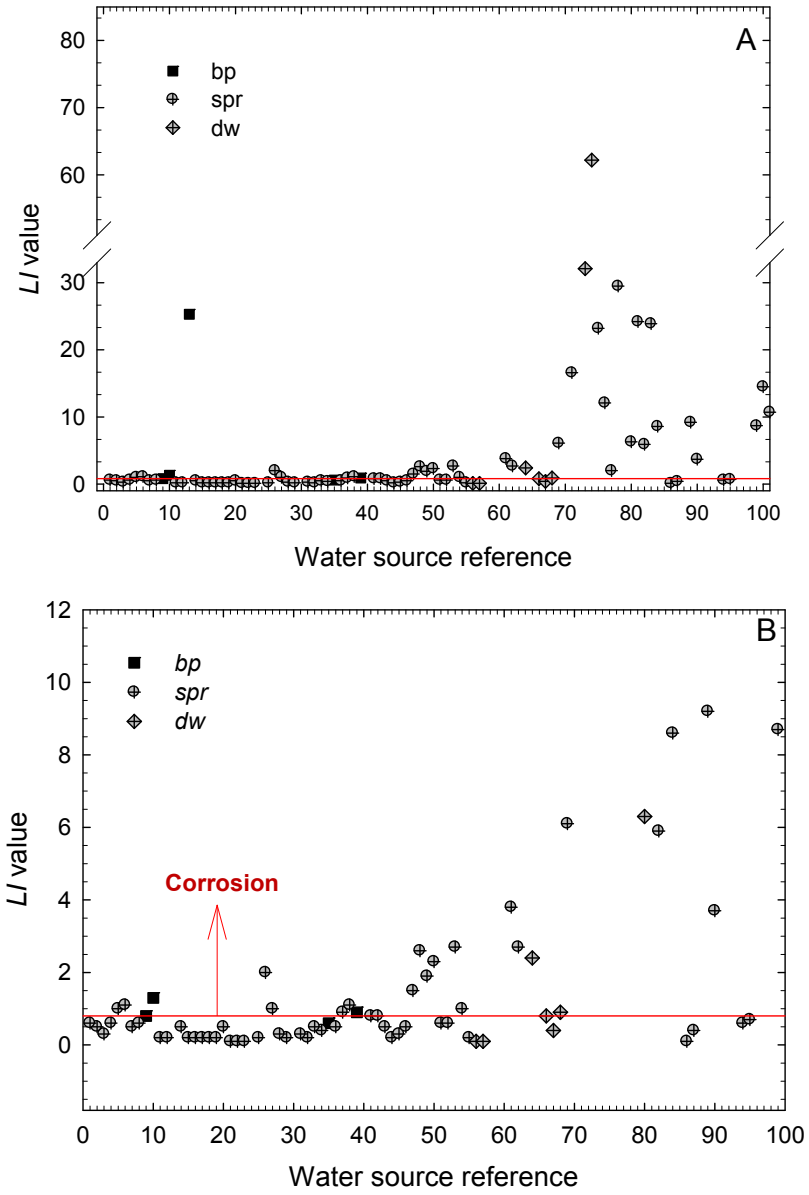


**Figure 5.** (**A**) Distribution of the water sources in the Azores archipelago according to their Larson–Skold Index (LI); and (**B**) Enlarged view of graph (**A**).

### *3.2. Determination of the Corrosive Action of the Natural Waters Using Electrochemical Measurements*

Though an estimate of the corrosive action of the natural waters could be derived in terms of the stability and scaling indexes described in the previous Section, the interpretation of these indexes must always be done with caution. Indeed, the method presents certain limitations arising from the different origin of the indexes. Thus, although corrosion rate estimates based on the Langelier Saturation and the Larson–Skold Indexes indeed possess some theoretical basis, the ranges taken on the base of the Puckorius Scaling and Ryznar Stability Indexes have been derived from observation. This fact indicates the need to quantify the aggressiveness of each water particularly against various metals, which can be used in installations of exploitation and/or recreation as well in pipes, by means of more direct techniques, namely from electrochemical measurements.

In this work, samples of three different thermal waters (corresponding to water sources of references AM3, AM9 and AM34) were taken as the test environment for the exposure of various typical metal systems. The methods employed were conventional corrosion tests based on the application of a potentiodynamic polarization to the samples. In brief, the electrical state of the metal samples was shifted from their spontaneously developed open circuit potential in the environment to monitor their subsequent electrochemical activation as a current flow through the electrochemical cell. Resistance polarization, Tafel plots and cyclic potentiodynamic polarization plots were sequentially recorded for each system. Figures 6 and 7 depict typical Tafel plots and cyclic polarization curves recorded for the various metals exposed to natural water taken from the water source of reference AM34. Similar measurements were performed for the other two waters (not shown). Corrosion parameters extracted from these measurements are listed in Table 4. They include the open circuit potential ($E_{cor}$), the corrosion current density ($j_{cor}$), anodic and cathodic Tafel slopes ($\beta_a$ and $\beta_c$, respectively), and the estimated corrosion rate ($r_{cor}$) expressed in millimeters of the material dissolved per year.

Measurements made with water from the AM9 source show high corrosion rates for the metal specimens that decrease in the sequence galvanized steel > carbon steel > zinc > copper > brass. In these cases, the obtained corrosion rates amounts some tens of micrometers per year, highlighting the high speed of corrosion of galvanized steel, which presents values of 130 $\mu m \cdot year^{-1}$. One order of magnitude smaller corrosion rates were determined in the case of Cr–Ni alloy and 304 grade stainless steel (namely a few micrometers per year), whereas the stainless steel 316L exhibited the highest corrosion resistance (with corrosion rates of hundredths of micrometers per year). These values are in accordance with the corrosion currents determined for each material. Thus, galvanized steel and carbon steel give high corrosion current densities amounting to 52.04 and 34.32 $\mu A \cdot cm^{-2}$, respectively, while 316L steel presents values of 0.057 $\mu A \cdot cm^{-2}$. The measurements of the corresponding open circuit potential values ($E_{cor}$) show the less noble values for Zn, galvanized steel and carbon steel, respectively, −1.022, −1.006, and −0.777 V *vs.* SCE. Stainless steel 316L is the only material that presents a rather noble value of $E_{cor}$, with an average value of −0.195 V *vs.* SCE.

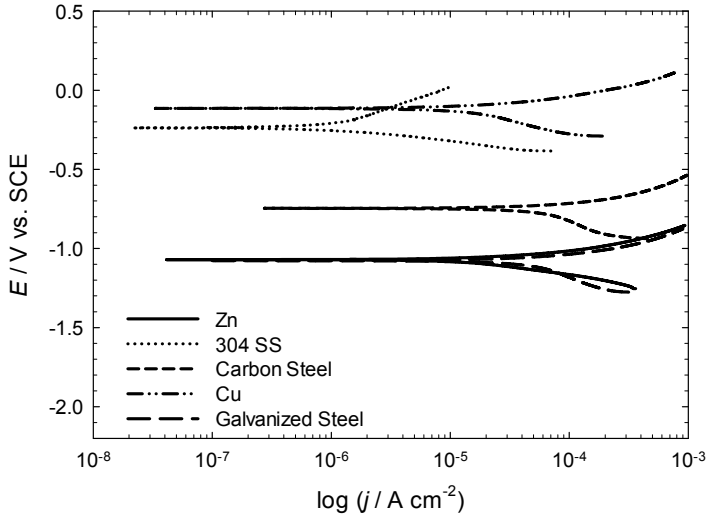


**Figure 6.** Tafel plots measured for various metal specimens during their immersion in thermal water taken from source AM34. Scan rate: 2 $mV \cdot s^{-1}$. Measurements were performed in the naturally aerated water at ambient temperature.

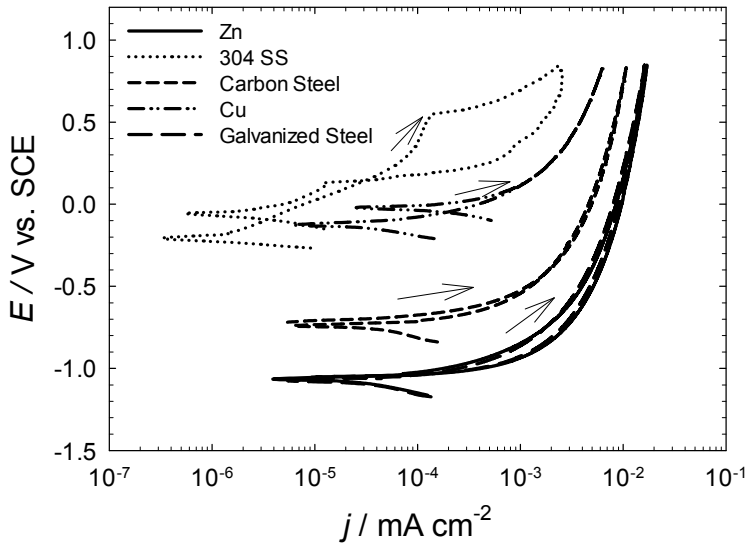


**Figure 7.** Cyclic polarization curves measured for various metal specimens during their immersion in thermal water taken from source AM34. Scan rate: 5 $mV \cdot s^{-1}$. Measurements were performed in the naturally aerated water at ambient temperature.

**Table 4.** Corrosion parameters obtained from potentiodynamic polarization experiments of indicated metals immersed in water samples taken from three springs in São Miguel Island.

| Metal | Water Source AM3 | | | | |
|---|---|---|---|---|---|
| | $E_{cor}$/mV *vs.* SCE | $j_{cor}$/μA·cm$^{-2}$ | $\beta_a$/mV | $-\beta_c$/mV | $r_{cor}$/mm·year$^{-1}$ |
| Zn | −1097.30 | 47.12 | 124.49 | 169.76 | 0.12 |
| Cu | −107.56 | 5.53 | 68.72 | 142.62 | $1.07 \times 10^{-2}$ |
| Cr–Ni | - | - | - | - | - |
| Brass | −118.87 | 5.73 | 54.32 | 112.38 | $1.10 \times 10^{-2}$ |
| Carbon Steel | −733.40 | 53.71 | 99.94 | 278.44 | 0.1 |
| Galvanized Steel | −1035.90 | 7.0 | 81.17 | 154.5 | $1.75 \times 10^{-2}$ |
| 304 SS | −112.18 | 0.33 | 217.16 | 85.83 | $5.74 \times 10^{-4}$ |
| 316L SS | −102.42 | 0.56 | 100.88 | 96.12 | $9.80 \times 10^{-4}$ |
| | **Water source AM9** | | | | |
| Zn | −1022.02 | 12.58 | 70.12 | 245.03 | $3.14 \times 10^{-2}$ |
| Cu | −142.64 | 10.32 | 83.2 | 271.62 | $1.99 \times 10^{-2}$ |
| Cr–Ni | −278.99 | 1.03 | 230.56 | 78.05 | $1.85 \times 10^{-3}$ |
| Brass | −182.76 | 8.28 | 56.03 | 115.62 | $1.59 \times 10^{-2}$ |
| Carbon Steel | −777.16 | 34.32 | 62.78 | 335.21 | $6.63 \times 10^{-2}$ |
| Galvanized Steel | −1006.10 | 52.04 | 114.0 | 647.54 | 0.13 |
| 304 SS | −276.44 | 0.99 | 304.83 | 72.2 | $1.71 \times 10^{-3}$ |
| 316L SS | −195.30 | $5.37 \times 10^{-2}$ | 181.02 | 46.29 | $9.32 \times 10^{-5}$ |
| | **Water source AM34** | | | | |
| Zn | −1075.74 | 15.44 | 65.76 | 104.77 | $3.85 \times 10^{-2}$ |
| Cu | −112.05 | 10.66 | 60.71 | 136.54 | $2.06 \times 10^{-2}$ |
| Cr–Ni | - | - | - | - | - |
| Brass | - | - | - | - | - |
| Carbon Steel | −750.63 | 50.29 | 97.01 | 221.34 | $9.72 \times 10^{-2}$ |
| Galvanized Steel | −1078.73 | 30.32 | 71.36 | 140.93 | $7.57 \times 10^{-2}$ |
| 304 SS | −228.79 | 1.11 | 257.16 | 92.09 | $1.92 \times 10^{-3}$ |

A similar behavior is observed with water samples AM3 and AM34. In this case, the metals order from the highest to the lowest corrosion rates present the sequence: Zn > carbon steel > galvanized steel > brass > Cu > 304 SS > 316L SS, with corrosion rates of the same order of magnitude that those detected for each material during exposure to water from source AM9. The corrosion rate of the Cr–Ni alloy could not be measured due to its high resistance to corrosion in these waters. The same applies to the water of the fountain AM34, where Cr–Ni alloys, brass and stainless steel 316L could not be measured due to its high resistance to corrosion in such environment. The trends of both the corrosion potential and the corrosion current densities in water samples AM3 and AM34 are similar than those observed for the water from the source AM9 (*cf.* Table 4). It must be noticed that the corrosion rate, current density and corrosion potential values determined for each system from the analysis of polarization resistance lines, from the Tafel plots and from the application of the Stern-Geary equation [23] were very similar.

The analysis of the cyclic polarization curves measured in water from the source AM9 show that no passivation occurs on Zn, Cu (where no active–passive transition is observed), carbon steel, brass, 304 and 316L stainless steels. Conversely, passivation occurs in the Cr-Ni alloy, associated to very small current densities, of the order of $10^{-4}$ A·cm$^{-2}$. These features match those derived from the Tafel plots. It is concluded that the highest corrosion resistance in water from source AM9 is 304 stainless steel, followed by the Cr–Ni alloy and then 316L stainless steel.

## 4. Conclusions

- The extension of the stability and scaling indexes commonly employed in the characterization of cooling waters in the industry to the characterization of natural waters from geothermal origin is satisfactory.
- The boiling pools, springs and drained wells present in the Archipelago of the Azores are mostly corrosive for structural metallic materials, as seen from the values obtained for the Langelier Saturation, Ryznar Stability, Puckorius Scaling, and Larson–Skold Indexes.
- According to the Langelier Saturation Index, more than 83% of the waters promote corrosion. By type of water, it has been found that the ratio of samples with corrosive characteristics amounts 87.7% for waters from springs (spr), 60% for waters from boiling pools (bp), and 72.7% of those from drained wells (dw). Yet, the values obtained for the hot springs (bp) must be taken only as indications because the high temperatures of these waters would require a more detailed study of their aggressiveness against those metals most commonly used for storing and piping.
- The preliminary electrochemical characterization of the corrosion rates of various metals of a wide industrial use in three water sources from São Miguel Island shows that the measured corrosion rates are very high for all the metals except 304 and 316 L stainless steels and the Cr–Ni alloy.
- These results provide a basis to initiate a combined electrochemical investigation of the aggressiveness of these natural waters both at higher temperatures as well as using condensed water collected from the boiling pools.

**Acknowledgments**

The authors wish to acknowledge the assistance of the Observatório Microbiano dos Açores (Furnas, São Miguel, Açores, Portugal), in particular to Joana Medeiros, in the collection of water samples from hot springs. This work was partially funded by the Ministerio de Economía y Competitividad (Madrid, Spain) and the European Regional Development Fund (Brussels, Belgium) under Project No. CTQ2012-36787. A grant awarded to Juan José Santana under the Unamuno Framework MAC/3/M126 of the European Regional Development Fund (Brussels, Belgium) to conduct a stay at the University of the Azores is gratefully acknowledged.

**Author Contributions**

Juan José Santana, Sergio González and Ricardo Manuel Souto conceived and designed the experiments; Juan José Santana and Bibiana María Fernández-Pérez performed the experiments and analyzed the data; Helena Cristina Vasconcelos contributed reagents/materials/analysis tools; Juan José Santana and Helena Cristina Vasconcelos wrote the paper with contributions from Sergio González and Ricardo Manuel Souto.

**Conflicts of Interest**

The authors declare no conflict of interest.

**References**

1. Aksoy, N.; Şimşek, C.; Gunduz, O. Groundwater contamination mechanism in a geothermal field: A case study. *J. Contam. Hydrol.* **2009**, *103*, 13–28.
2. Guo, Q.; Wang, X.; Liu, W. Hydrogeochemistry and environmental impact of geothermal waters from Yangyi of Tibet, China. *J. Volcanol. Geotherm. Res.* **2009**, *180*, 9–20.
3. Aiuppa, A.; Allard, P.; D'Alessandro, W.; Michel, A.; Parello, F.; Treuil, M.; Valenza, M. Mobility and fluxes of major, minor and trace metals during basalt weathering and groundwater transport at Mt. Etna Volcano (Sicily). *Geochim. Cosmochim. Acta* **2000**, *64*, 1827–1841.
4. Custódio, E. Groundwater characteristics and problems in volcanic rock terrains. In *Isotopic Techniques in the Study of the Hydrology of Fractures and Fissured Rocks*; IAEA: Vienna, Austria, 1989; pp. 87–137.
5. Cruz, J.V.; Silva, M.O. Groundwater salinisation in Pico Island (Azores, Portugal): Origin and mechanisms. *Environ. Geol.* **2000**, *39*, 1181–1189.
6. Cruz, J.V.; Silva, M.O. Hydrogeologic framework of the Pico Island (Azores, Portugal). *Hydrogeol. J.* **2001**, *9*, 177–189.
7. Kim, Y.; Lee, K.-S.; Koh, D.-C.; Lee, D.-H.; Lee, S.-G.; Park, W.-B.; Koh, G.-W.; Woo, N.-C. Hydrogeochemical and isotopic evidence of groundwater salinization in a coastal aquifer: A case study in Jeju volcanic island, Korea. *J. Hydrol.* **2003**, *270*, 282–294.
8. Brusca, L.; Aiuppa, A.; D'Alessandro, W.; Parello, F.; Allard, P.; Michel, A. Geochemical mapping of magmatic gas-water-rock interactions in the aquifer of Mount Etna volcano. *J. Volcanol. Geotherm. Res.* **2001**, *108*, 199–218.

9. Federico, C.; Aiuppa, A.; Allard, P.; Bellomo, S.; Jean-Baptiste, P.; Parello, F.; Valenza, M. Magma-derived gas influx and water-rock interaction in the volcanic aquifer of Mt. Vesuvius, Italy. *Geochim. Cosmochim. Acta* **2002**, *66*, 963–981.
10. Cruz, J.V.; Coutinho, R.M.; Carvalho, M.R.; Oskarsson, N.; Gislason, S.R. Chemistry of waters from Furnas volcano, São Miguel, Azores: Fluxes of volcanic carbon dioxide and leached material. *J. Volcanol. Geotherm. Res.* **1999**, *92*, 151–167.
11. Cruz, J.V.; França, Z. Mineral and thermal waters in the Azores archipelago (Portugal): Geological setting and hydrogeochemical outline. In Proceedings of the XXXI IAH Congress—New Approaches to Characterising Groundwater Flow, Munich, Germany, 10–14 September 2001; Seiler, K.-P., Wohnlich, S., Eds.; Balkema Publishers: Lisse, The Netherlands, 2001; pp. 477–481.
12. Cruz, J.V. Groundwater and volcanoes: Examples from the Azores archipelago. *Environ. Geol.* **2003**, *44*, 343–355.
13. Cruz, J.V.; França, Z. Hydrogeochemistry of thermal and mineral springs of the Azores archipelago (Portugal). *J. Volcanol. Geotherm. Res.* **2006**, *151*, 382–398.
14. Carvalho, M.R.; Forjaz, V.H.; Almeida, C. Chemical composition of deep hydrothermal fluids in the Ribeira Grande geothermal field (São Miguel, Azores). *J. Volcanol. Geotherm. Res.* **2006**, *156*, 116–134.
15. Morell, I.; Pulido Bosch, A.; Daniele, L.; Cruz, J.V. Chemical and isotopic assessment in volcanic thermal waters: Cases of Ischia (Italy) and São Miguel (Azores, Portugal). *Hydrol. Process.* **2008**, *22*, 4386–4399.
16. Cruz, J.V.; Freire, P.; Costa, A. Mineral waters characterization in the Azores archipelago (Portugal). *J. Volcanol. Geotherm. Res.* **2010**, *90*, 353–364.
17. Langelier, W.F. Chemical equilibria in water treatment. *J. Am. Water Works Assoc.* **1946**, *38*, 169–178.
18. Ryznard, J.W. A new index for determining amount of calcium carbonate scale formed by a water. *J. Am. Water. Works Assoc.* **1944**, *36*, 472–486.
19. Puckorius, P.R.; Loretitsch, G.R. Cooling water scale and scale indices: What they mean—How to use them effectively—How they can cut treatment costs, IWC 99–47. In Proceedings of the International Water Conference, Pittsburgh, PA, USA, 18 October 1999; pp. 378–387.
20. Puckorius, R.; Brooke, J.M. A new practical index for calcium carbonate scale prediction in cooling systems. *Corrosion* **1991**, *47*, 280–284.
21. Larson, T.E.; Skold, R.V. *Laboratory Studies Relating Mineral Quality of Water to Corrosion of Steel and Cast Iron*; ISWS C-71; Illinois State Water Survey: Champaign, IL, USA. 1958; pp. 43–46.
22. W-index-Spreadsheet, Marvin Silbert and Associates. Available online: http://www.silbert.org/main_msa.html (accessed on 4 March 2015).
23. Tait, W.S. *An Introduction to Electrochemical Corrosion Testing for Practicing Engineers and Scientists*; PairODocs Publications: Racine, WI, USA, 1994; pp. 43–77.